

# The Triplet–Singlet Gap in the *m*-Xylylene Radical: A Not So Simple One

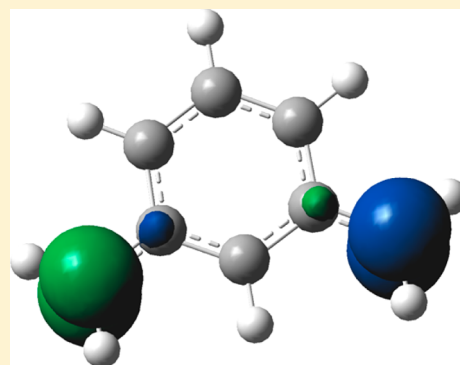
Daniel Reta Mañeru,<sup>†</sup> Arun K. Pal,<sup>‡</sup> Ibério de P. R. Moreira,<sup>†</sup> Sambhu N. Datta,<sup>‡</sup> and Francesc Illas<sup>\*,†</sup>

<sup>†</sup>Departament de Química Física & Institut de Química Teòrica i Computacional (IQTCUB), Universitat de Barcelona, C/Martí i Franquès 1, E-08028 Barcelona, Spain

<sup>‡</sup>Department of Chemistry, Indian Institute of Technology, Bombay, Powai, Mumbai 400076, India

## S Supporting Information

**ABSTRACT:** *Meta*-benzoquinodimethane (MBQDM) or *m*-xylylene provides a model for larger organic diradicals, the triplet–singlet gap being the key property. In the present work this energy difference has been the object of a systematic study by means of several density functional theory-based methods including B3LYP, M06, M06-2X, HSE and LC- $\omega$ PBE potentials and a variety of wave function-based methods such as complete active space self consistent field (CASSCF), Multireference second-order Møller–Plesset (MRMP), difference dedicated configuration interaction (DDCI), and Multireference configuration interaction (MRCI). In each case various basis sets of increasing quality have been explored, and the effect of the molecular geometry is also analyzed. The use of the triplet and broken symmetry (BS) solutions for the corresponding optimized geometries obtained from B3LYP and especially M06-2X functionals provide the value of the adiabatic triplet–singlet gap closer to experiment when compared to the reported value of Wenthold, Kim, and Lineberger, (*J. Am. Chem. Soc.* **1997**, *119*, 1354) and also for the electron affinity. The agreement further improves using the full  $\pi$ -valence CASSCF(8,8) optimized geometry as an attempt to correct for the spin contamination effects on the geometry of the BS state. The CASSCF, MRMP, and MRCI, even with the full  $\pi$  valence CAS(8,8) as reference and relatively large basis set, systematically overestimate the experimental value indicating either that an accurate description must go beyond this level of theory, including  $\sigma$  electrons and higher order polarization functions, or perhaps that the measured value is affected by the experimental conditions.



## 1. INTRODUCTION

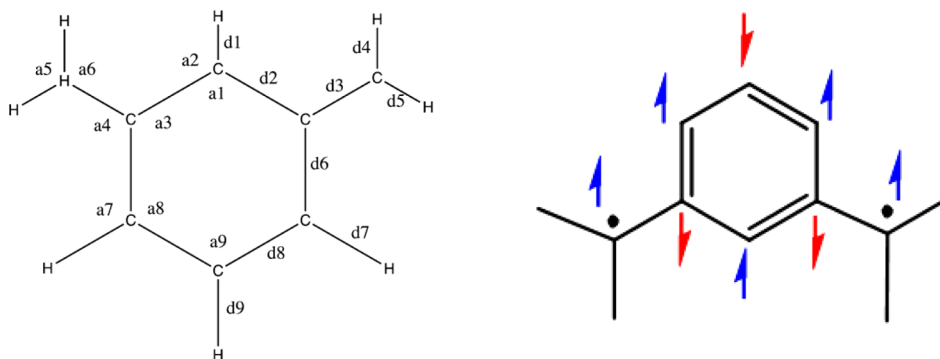
Apart from the obvious interest in general organic chemistry,<sup>1</sup> organic diradicals constitute an invaluable set of systems to investigate chemical reactivity and molecular mechanisms.<sup>2</sup> Along the years, several experimental techniques such as matrix isolation<sup>3</sup> and flash photolysis<sup>4,5</sup> allowed the synthesis of these generally short-lived species. Further developments allowed the spectroscopic characterization of diradicals and, in particular, negative ion photoelectron spectroscopy (NIPES) has been shown to be a very useful tool to scrutiny their electronic structure.<sup>6</sup> A second field of interest related to diradicals is their possible application in magnetic technologies.<sup>7,8</sup> Here, the energy difference between low-lying states of different multiplicity, usually singlet and triplet states, becomes the key property and efforts have been made to synthesize diradicals with tuned triplet–singlet gaps and, more specifically, to obtain diradicals with a triplet ground state which can be used in magnetic devices. Most of the organic radicals, diradicals, and polyradicals are highly conjugated systems, in contrast to metal complexes or clusters. For such conjugated species, the Borden–Davidson disjoint SOMO dictum<sup>9</sup> and the spin alternation principle<sup>10,11</sup> in unrestricted SCF calculations<sup>12,13</sup> of Kohn–Sham form have been found to be highly successful in the prediction of triplet ground states. Clearly, the accurate

prediction of triplet–singlet gaps in organic diradicals is of paramount importance.<sup>14–17</sup> Several theoretical methods have been proposed including those based on different density functional theory (DFT)-based method and those based in wave function theory. A brief summary of the different methods and their performance for metal complexes and similar systems can be found in several recent reviews<sup>18,19</sup> and specialized articles.<sup>20</sup>

Among the different known rather stable diradicals, *meta*-benzoquinodimethane (MBQDM) or *m*-xylylene (Scheme 1) has been considered as a benchmark because it is well characterized from experiment. In fact, Platz et al.<sup>21</sup> have synthesized MBQDM and used electron spin resonance (ESR) to provide the first evidence of the triplet character of its electronic ground state. The molecular structure of MBQDM exhibits  $C_{2v}$  symmetry and the open-shell orbitals  $a_1$  and  $b_2$  character so that the electronic ground state can be denoted as  $^3B_2$ . Later on, Wenthold et al.<sup>22</sup> provided an accurate estimate of the electron affinity of this diradical, and their NIPES study has shown that the low-lying electronic states are  $^1A_1$  and  $^1B_2$ , respectively. Note that both electronic states have a strong

Received: October 9, 2013

Published: December 10, 2013

Scheme 1. Schematic Representation of the Molecular Structure of *m*-Xylylene<sup>a</sup>

<sup>a</sup>Bond angles and lengths are named. The spin alternation scheme is explicitly illustrated indicating the diradical to be a ground-state triplet.

open-shell character and that the  $^1A_1$  cannot be represented by a single closed-shell Slater determinant. The order of the electronic states is well predicted by theoretical arguments and appropriate ab initio calculations.<sup>23</sup> The electronic structure of this and other diradicals has also been reviewed in a recent perspective paper.<sup>24</sup> Note, however, that previous studies using approximate but rather extended configuration interaction wave function in the  $\pi$  space predicted a quite large effect of the quadruple excitations on a single reference,<sup>25</sup> which can be taken as a first indication of the subtleties hidden in the electronic structure of this kind of diradical; we will come back to this point later on.

An additional puzzling aspect with the electronic structure of MBQDM, however, is that photoelectron spectroscopy exhibits an adiabatic character as the spectra display a vibrational fine structure which is also resolved. To understand the experiment is convenient to consider the illumination of a doublet anion by light. The photon has enough energy ( $h\nu$ ) to eject one electron. The remaining neutral species is left in its vibronic states. The energy difference ( $h\nu - KE_{\max}$ ), where  $KE_{\max}$  is the maximum kinetic energy of the electron equals the energy between the neutral molecule and the negative ion, that is, the electron affinity of the neutral species. It transpires that the NIPES spectrum will give the relative energies of the adiabatic ground states with different spin. Because the  $KE_{\max}$  spectrum shows vibrational structure, the NIPES data can be interpreted for the adiabatic coupling constant, with zero-point vibrational energy correction. This is also consistent with the fact that agreement between experiment and theory is better reproduced by considering adiabatic transitions<sup>23</sup> as explained in detail below. The agreement between experiment and theory is, however, only moderate since the multireference second-order perturbation theory (CASPT2) calculations of Hrovat et al.,<sup>23</sup> using a complete active space self consistent field (CASSCF) reference with eight electrons and eight orbitals, hereafter referred to as CAS(8,8), defining the complete active space, predict an adiabatic triplet–singlet gap of 11.7 kcal mol<sup>-1</sup> (4092 cm<sup>-1</sup>)—11.0 kcal mol<sup>-1</sup> or 3850 cm<sup>-1</sup> after correcting for the zero-point energy (ZPE) using the CASSCF vibrational frequencies—while the experimental value is of  $9.6 \pm 0.2$  kcal mol<sup>-1</sup> ( $3358 \pm 70$  cm<sup>-1</sup>). The absolute error of 2.1 kcal mol<sup>-1</sup> or 734 cm<sup>-1</sup> (492 cm<sup>-1</sup> if ZPE corrected), while modest in absolute terms, still represents a relative large error of 22%, and one may wonder whether a more accurate value can be obtained by improving the level of theory. For instance, the value reported by Hrovat et al.<sup>23</sup> has been obtained using the geometry optimized of each state at the 6-31G\*/CASSCF level

with a CAS(8,8). In principle, the basis set quality can be easily improved which can affect the equilibrium geometry of the two electronic states. It is also convenient to explore the value corresponding to a Franck–Condon transition which would provide information about the effect of geometry relaxation in the excited state. Vertical and adiabatic excitation energies have been reported by Wang and Krylov<sup>26</sup> using the equation of motion spin-flip coupled cluster singles and doubles (EOM-SF-CCSD) method and a larger basis set (6-311G(2d) for C and 6-31G\* for H). The reported values are 13.8 kcal mol<sup>-1</sup> (4839 cm<sup>-1</sup>) and 11.3 kcal mol<sup>-1</sup> (3952 cm<sup>-1</sup>) for the vertical and adiabatic transitions, respectively. In this case, the difference between vertical and adiabatic values is significantly large, 2.5 kcal mol<sup>-1</sup> or almost 900 cm<sup>-1</sup>. There is a modest improvement over the CASPT2 values of Hrovat et al.,<sup>23</sup> and an 18% error with respect to experiment still remains.

From a more fundamental point of view, it is also important to note that for a diradical such as MBQDM, one would expect a minimal CAS(2,2) description to be sufficient. This is the case for several organic diradicals and also for Cu dinuclear and similar magnetic inorganic complexes where CASPT2 or DDCI calculations carried out using a minimal CAS(2,2) reference space predict excellent values of the triplet–singlet gap or equivalently of the magnetic coupling constant which happens to be a more appropriate term when the energy difference is very small.<sup>18,27</sup> Very recently Suaud et al.<sup>28</sup> have analyzed this problem in detail and found that the description based on a CAS(2,2) fails for MBQDM. They attribute the failure to the too localized character of the singly occupied orbitals in the CASSCF(2,2) wave function and develop an iterative procedure to improve the orbitals based on natural orbitals. These authors use geometries for singlet and triplet optimized using the EOM-SF-CCSD method as reported by Wang and Krylov.<sup>26</sup> The best value obtained by these authors for the adiabatic triplet–singlet gap restricted to a CAS(2,2) model is 12.4 kcal mol<sup>-1</sup> (4355 cm<sup>-1</sup>), comparable to their CASPT2 value of 10.8 kcal mol<sup>-1</sup> (3790 cm<sup>-1</sup>) obtained using the EOM-SF-CCSD structures and a CASSCF(8,8) reference. This value is clearly too large, indicating the difficulty to project the physics into the minimal CAS space. The CASPT2 value, obtained using a CASSCF(8,8) reference, a 6-31G\*\* and the geometry from the EOM-SF-CCSD calculations are in better agreement with experiment, the relative error being reduced to 13%.

The discussion above shows evidence of the delicate interplay between, structure, basis set, and description of electron correlation in defining the triplet–singlet gap of

MBQDM which calls for a more systematic study. On the other hand, one must also realize that this type of CASSCF/CASPT2 calculations become rapidly intractable when the size of the molecule increases, even moderately. DFT-based calculations offer a very attractive alternative, and there is abundant literature in related systems indicating that the popular B3LYP and similar hybrid functionals tend to provide values close to the experimental one,<sup>29–37</sup> although the semiempirical flavor of hybrid functionals makes one wonder if the right answer comes from the right reason, a long-standing question in modern electronic structure theory. Nevertheless, the complexity of the electronic structure of MBQDM revealed by the CASPT2 and EOM-SF-CCSD calculations commented above may also appear to be difficult for DFT-based methods. In the present work, we provide a systematic study of the triplet–singlet gap of MBQDM using a variety of wave function- and DFT-based methods covering different types of active spaces and several configuration interaction approaches, various types of basis sets ranging from standard Pople’s basis to correlation consistent sets, different exchange–correlation functionals, and carefully exploring the effect of the geometry in the vertical and adiabatic triplet–singlet gap of this not so simple organic diradical.

## 2. COMPUTATIONAL DETAILS

The triplet–singlet gap of MBQDM has been studied at various levels of theory, including several wave function and DFT methods, as specified in detail below. In these calculations all electrons have been explicitly considered and the corresponding one electron states, molecular or Kohn–Sham, expanded in Gaussian type basis sets of increasing size. Two families of basis sets have been used, the first one follows the well-known approach developed by Pople and co-workers<sup>38,39</sup> which is broadly used in all sorts of applications, and the second one follows the approach of Dunning for correlations consistent basis sets,<sup>40</sup> especially designed to be used in explicitly correlated calculations. For the first set, we start with the 6-31G\* double- $\zeta$  plus polarization standard basis, the 6-31G\*\* including a polarization in the H atoms,<sup>41</sup> the 6-311G\*\* and 6-311++G\*\* triple- $\zeta$  basis plus polarization sets, the latter including also diffuse functions,<sup>42</sup> and the more extended 6-311++G(3df3pd).<sup>43</sup> For the second one we used the aug-cc-pVDZ and the aug-cc-pVTZ sets.<sup>40,44</sup>

For the DFT-based methods a number of state of the art exchange–correlation potentials have been used starting with the popular B3LYP hybrid method<sup>45</sup> and including the M06 and M06-2X meta hybrid functionals of Zhao and Truhlar<sup>46–48</sup> and the short-range HSE<sup>49</sup> and long-range LC- $\omega$ PBE<sup>50</sup> range separated functionals. Note, however, that the standard Kohn–Sham implementation of DFT does not allow treating open-shell systems in a rigorous way<sup>51,52</sup> and some alternative approaches such as restricted ensemble Kohn–Sham (REKS)<sup>53,54</sup> and, more recently, spin flip time-dependent DFT (SF-TDDFT)<sup>55</sup> methods have been proposed and applied to similar problems where the quantity of interest is a triplet–singlet energy difference.<sup>56,57</sup> In the present work we make use of the standard spin unrestricted Kohn–Sham formalism, where a high-spin Kohn–Sham determinant with two unpaired electrons with parallel spin is used to represent the triplet state and a broken symmetry (BS)<sup>58–60</sup> solution is used to obtain the energy of the singlet<sup>61</sup> using the formula proposed by Yamaguchi.<sup>62–64</sup> In this way, the vertical DFT triplet–singlet gap is approximately twice the energy difference between the high spin and the BS solutions. It is also worth pointing out

that, for a given functional, triplet–singlet gaps computed using spin projection are in good agreement with those obtained from the SF-TDDFT methods where spin states are properly represented.<sup>57</sup>

The case of adiabatic transitions requires some additional comments. In fact, it is important that the Yamaguchi’s approach is well-defined for a given geometry, either singlet (S), triplet (T) approximated by the high-spin state or BS obtained from the appropriate method. Following Yamaguchi<sup>62–64</sup> one can obtain the vertical triplet–singlet gap (triplet to singlet excitation energy)  $\Delta_{TS}^i$  (or simply  $\Delta_{\text{vert}}^i$ ) at a given geometry  $i$  as

$$\Delta_{TS}^i \equiv \Delta_{\text{vert}}^i = E_{S^i} - E_{T^i} = \frac{2(E_{BS^i} - E_{T^i})}{\langle S_{T^i}^2 \rangle - \langle S_{BS^i}^2 \rangle} \quad (1)$$

where  $E_{S^i}$ ,  $E_{T^i}$  and  $E_{BS^i}$  are the energy of the singlet, triplet, and BS solution, respectively, and the superindex “ $i$ ” is used to indicate the geometry used in the calculations. The denominator contains the expectation value of the square of the total spin operator for the triplet and BS solutions (close to 2.000 and 1.000, respectively) and, again, the superindex indicates the molecular geometry. Obviously, the expectation value of the square of the total spin operator has been obtained from the electron density for the reference Kohn–Sham system. From eq 1 it is possible to not only calculate  $\Delta_{TS}^i$  but also to estimate the energy of the (decontaminated) open-shell singlet  $E_{S^i}$  as

$$E_{S^i} = \frac{2(E_{BS^i} - E_{T^i})}{\langle S_{T^i}^2 \rangle - \langle S_{BS^i}^2 \rangle} + E_{T^i} \quad (2)$$

which is required to obtain the adiabatic triplet–singlet gap  $\Delta_{TS}^{\text{adia}}$  (or simply  $\Delta_{\text{adia}}$ ) as

$$\Delta_{TS}^{\text{adia}} \equiv \Delta_{\text{adia}} = E_{S^j} - E_{T^j} = \frac{2(E_{BS^j} - E_{T^j})}{\langle S_{T^j}^2 \rangle - \langle S_{BS^j}^2 \rangle} + E_{T^j} - E_{T^i} \quad (3)$$

where  $i$  and  $j$  refer now to the molecular geometry of the singlet, usually taken as that predicted from the BS approach, and of the triplet, respectively. Note, however, that one could use the geometry of the open-shell singlet as predicted by the appropriate method. In the next section we will come back to this point in some more detail. For practical purposes one may approximate eq 3 as

$$\Delta_{TS}^{\text{adia,approx}} \equiv \Delta_{\text{apadia}} = E_{S^j} - E_{T^j} = \frac{2(E_{BS^j} - E_{T^j})}{\langle S_{T^j}^2 \rangle - \langle S_{BS^j}^2 \rangle} \quad (4)$$

which does not require the calculation of the energy of triplet state at the BS (or singlet) geometry. Note, however, that use of eq 4 may lead to inaccurate values if the geometry of the two states differs significantly.

Finally, a number of explicitly correlated wave function methods have been explored, all starting from a CASSCF reference but with the CAS varying from the minimal (2,2) description to the CAS(8,8) full  $\pi$  valence. Next, dynamical correlation is included through the second-order multireference Møller–Plesset (MRMP) perturbation theory<sup>65–68</sup> and, in some cases, through fully variational multireference single and doubles configuration interaction (MRSDCI). A series of calculations using the difference dedicated configuration interaction (DDCI)<sup>69</sup> method have also been carried out starting from different CAS as reference. The DDCI leads to a

**Table 1. Vertical and Adiabatic Triplet–Singlet ( $\Delta_{\text{vert}}$  and  $\Delta_{\text{adia}}$ ) Gap of *m*-Xylylene As Predicted from Different DFT-Based Methods Using Basis Sets of Increasing Size<sup>a</sup>**

cm <sup>-1</sup>	6-311++G**			6-31G**			6-31G*		
	$\Delta_{\text{vert}}$	$\Delta_{\text{apadia}}$	$\Delta_{\text{adia}}$	$\Delta_{\text{vert}}$	$\Delta_{\text{apadia}}$	$\Delta_{\text{adia}}$	$\Delta_{\text{vert}}$	$\Delta_{\text{apadia}}$	$\Delta_{\text{adia}}$
B3LYP	4564	4256	4133	4753	4430	4304	4773	4444	4320
M06	5100	4828	4679	5329	4948	4789	5361	4966	4812
M06-2X	4142	3755	3615	4100	3706	3566	4096	3697	3560
HSE	5097	4719	4576	5270	4881	4735	5293	4897	4753
LC- $\omega$ PBE	7371	6439	6185	7534	6600	6340	7551	6617	6356

<sup>a</sup>In order to separate geometric effects, all values have been computed using the optimized structure as obtained with the 6-311G\*\* basis set for each method.

**Table 2. Total Energy and  $\langle S^2 \rangle$ , Both in Atomic Units, Vertical and Adiabatic Triplet–Singlet ( $\Delta_{\text{vert}}$  and  $\Delta_{\text{adia}}$ ) Gap As Predicted From UB3LYP and UM062X Functionals Using 6-311++G(3df,3pd) Basis Set<sup>a</sup>**

system	state/geom	B3LYP		M062X	
		E	$\langle S^2 \rangle$	E	$\langle S^2 \rangle$
<i>m</i> -xylylene diradical	T/T	−309.6905204	2.063121	−309.5325703	2.069032
	BS/T	−309.6796469	1.012419	−309.5226956	1.018404
	$\Delta_{\text{vert}}$	4542		4126	
	T/BS	−309.689707	2.060854	−309.5317944	2.064708
	BS/BS	−309.6803489	1.011834	−309.5235966	1.017800
<i>m</i> -xylylene anion	$\Delta_{\text{adia}}$	4127		3607	
	D/D	−309.7193305	0.781376	−309.5619826	0.786878

<sup>a</sup> $\Delta_{\text{vert}}$  and  $\Delta_{\text{adia}}$  values in cm<sup>-1</sup> are also reported. T = triplet, D = doublet, BS = broken symmetry.

configuration interaction expansion which is a subset of the full MRSDCI, neglecting the 2h–2p (h = hole; p = particle) excitations involving orbitals out of the CAS which at second order of perturbation theory equally contribute to the two states, provided the same set of molecular orbital is used.<sup>70</sup> In the case of CAS(8,8), the resulting MRSDCI expansion is too large to be explicitly treated, and a selection procedure has been carried out based on the weight of the configurations in the CASSCF wave function. Here it is important to point out that DDCI and MRSDCI wave functions, as any truncated CI expansion, suffer from the normalization error, and this may introduce some uncertainty in the calculated excitation energy values. Nevertheless, these methods are often the choice for studies involving excited states, and the accuracy in calculated excitation energies is usually below 500 cm<sup>-1</sup>.<sup>71–73</sup> Note, however, that in the case of magnetic coupling constants of dinuclear complexes, the values predicted by the DDCI method are often within 50–100 cm<sup>-1</sup> of the experimental values.<sup>74</sup>

In order to explore the effect of the geometry separately, single point energy calculations have been carried out for the singlet and triplet states at the geometry optimized by different methods either of DFT or wave function type and by employing several of the basis sets described above. Vertical and adiabatic transitions have been obtained, and the pertinent optimized structures, total energy values, and other relevant data are collected in the Supporting Information file.

The DFT-based calculations have been carried out using the Gaussian09 suite of programs;<sup>75</sup> CASSCF and MRMP calculations were run with the GAMESS06 code<sup>76,77</sup> and, finally, DDCI and selected CI calculations were carried out using the CASDI code<sup>78</sup> interfaced to the MOLCAS7.6 package<sup>79</sup> which provided the CASSCF reference wave functions. Here it is important to point out that MRMP has some important differences with the broadly used CASPT2 method<sup>80,81</sup> regarding the states used to span the first-order wave function. In CASPT2, single and double excitations are

applied to the reference wave CASSCF function, while in MRPT all singly and doubly excited determinants obtained from each of the determinants in the reference wave function are considered. In other words, CASPT2 uses a contracted reference function, whereas MRPT does not. The use of a contracted/uncontracted reference may be advantageous depending on the particular case, although there is not a general rule. An alternative, possibly better, option might consist in using the NEVPT2 formalism of Malrieu et al.<sup>82</sup> which uses a different partition of the Hamiltonian which has some formal and practical advantages, it avoids the problem of intruder states although these do not appear here. In any case one must keep in mind that CASPT2, MRMP, and NEVPT2 are second-order approaches and that higher order terms, which can make important contributions, are missing.

### 3. THE EFFECT OF BASIS SET, GEOMETRY, AND METHOD

In order to separate effects arising from the choice of the method, the choice of the basis set, and the influence of the geometry, a series of calculations have been carried out which use the same geometry with different basis set and a given method or the optimum geometry with different basis sets and different methods. For simplicity, the results of DFT calculations will be described first.

#### 3.1. Influence of the Basis Set and Exchange–Correlation Potential in the DFT-Based Calculations.

First, we explore the effect of the basis set on the calculation of the triplet–singlet gap by taking the geometry optimized for the triplet and BS states for each density functional with the 6-311G\*\* basis set and evaluate the energy with different basis sets. Results in Table 1 for the vertical, approximated adiabatic, and adiabatic triplet–singlet gap ( $\Delta_{\text{vert}}$ ,  $\Delta_{\text{apadia}}$ , and  $\Delta_{\text{adia}}$ ), respectively, allow one to extract several conclusions. In general the  $\Delta_{\text{apadia}}$  values follow the trends of  $\Delta_{\text{adia}}$  but are less accurate.



**Table 3.** Vertical and Adiabatic Triplet–Singlet ( $\Delta_{\text{vert}}$  and  $\Delta_{\text{adia}}$ ) Gap of *m*-Xylylene As Predicted from Different DFT-Based Methods<sup>a</sup>

cm <sup>−1</sup>	B3LYP		HSE		M06		M06-2X		$\mu \pm \sigma$	
	$\Delta_{\text{vert}}$	$\Delta_{\text{adia}}$	$\Delta_{\text{vert}}$	$\Delta_{\text{adia}}$	$\Delta_{\text{vert}}$	$\Delta_{\text{adia}}$	$\Delta_{\text{vert}}$	$\Delta_{\text{adia}}$	$\Delta_{\text{vert}}$	$\Delta_{\text{adia}}$
B3LYP	4564	4133	4503	4092	4600	3996	4405	4052	4518 ± 74	4068 ± 51
M06	5067	4585	4994	4529	5100	4679	4884	4483	5011 ± 83	4569 ± 73
M06-2X	4324	3726	4255	3665	4370	3718	4142	3615	4273 ± 86	3681 ± 45
HSE	5166	4633	5097	4576	5207	4637	4985	4528	5114 ± 84	4594 ± 45

<sup>a</sup>The values have been obtained from calculations using the 6-311++G\*\* basis set and the optimized structure, either for triplet or singlet, obtained with the 6-311G\*\* basis set for each method. The different columns indicate the origin of the geometry, and the rows report calculated values at the different structures. Mean values ( $\mu$ ) and standard deviation ( $\sigma$ ) are provided in the rightmost columns.

Therefore, they are presented in Table 1 for completeness but are not further discussed. The adiabatic ( $\Delta_{\text{adia}}$ ) values are always closer to experiment, and the difference between vertical and adiabatic calculated excitations is roughly 400 cm<sup>−1</sup> rather irrespective of the method and basis used. Likewise, the effect of the density functional is much larger than the effect of the basis set. For instance, for the B3LYP functional the  $\Delta_{\text{vert}}$  value goes from 4564 to 4773 cm<sup>−1</sup> when decreasing the basis set from 6-311++G\*\* to the much less extended 6-31G\*; a change of 200 cm<sup>−1</sup> that is certainly not negligible. However, the use of M06-2X instead of B3LYP while keeping the 6-311++G\*\* basis set leads to a change of more than 400 cm<sup>−1</sup>. The change is even larger if one considers the range separated functionals. In this respect, it is surprising to find that the LC- $\omega$ PBE performs quite badly, especially because this functional was parametrized for thermochemistry and barrier heights of main group molecules.<sup>50</sup> This functional, however, led to excellent results in the case of the triplet–singlet gap in Cu dinuclear complexes<sup>83</sup> and the superconducting cuprates parent compounds.<sup>84</sup> The LC- $\omega$ PBE results will not be commented in the forthcoming sections.

In order to further check the effect of the basis set we comment on the results obtained with the largest set, the 6-311++G(3df,3pd), and with the B3LYP and M06-2X functional as shown in Table 2. The calculated  $\Delta_{\text{adia}}$  values are 4127 and 3607 cm<sup>−1</sup>, respectively, which correspond to changes of only 6 cm<sup>−1</sup> (B3LYP) and 8 cm<sup>−1</sup> (M06-2X) with respect to values computed with the 6-311++G\*\* basis set. Therefore, it is possible to consider the values thus obtained as effectively converged. Note, in addition that while the B3LYP value exhibits a 23% error with respect to experiment, the M06-2X one displays a much smaller error of 7% only, surprisingly better than the more computationally demanding EOM-SF-CCSD calculations and also better than CASPT2 with a CAS(8,8) reference. Clearly, the weakness of the DFT methods is that to a priori predict which of the plethora of available functionals is appropriate for the problem of interest is nearly impossible. However, one may safely rely on the time-tested B3LYP and the more modern M06-2X, at least to get a qualitatively correct guidance.

**3.2. Influence of the Geometry in the DFT-Based Calculations.** Results in the previous subsection clearly show that the calculated triplet–singlet gap largely depends on the exchange–correlation potential. This is not surprising, as it has been recognized long ago for a variety of magnetic systems, mostly dinuclear complexes or magnetic solids as fluorides or cuprates.<sup>18,57,61</sup> Here, the energy difference between the two states is more in the range of optical excitations, but nonetheless, the main features remain practically the same except for a less localized character of the open-shell orbitals in

MBQDM which has significant implications in the wave function description. In the case of dinuclear complexes or magnetic solids, it is customary to explore the different electronic states of interest at the experimental geometry, which is available from experiment,<sup>57</sup> mainly through X-ray diffraction. In the case of organic diradicals the situation is different since the species are short-lived and structural determination becomes extremely difficult.

Theoretical methods provide an alternative approach to structure determination, even for short-lived species, and most DFT-based methods provide reliable structures.<sup>85</sup> However, the fact that the triplet–singlet gap is so sensitive to the exchange–correlation potential raises questions about whether the molecular structure is a crucial point. This is also relevant to explicitly correlated wave function-based methods for which geometry optimization can be extremely time-consuming. In order to disentangle molecular structure from energy evaluation, we have carried out a series of calculations where, in a first step, the geometry of the triplet and singlet (BS) states of MBQDM is obtained with the different DFT methods used in the present work and using a 6-311G\*\* basis set. In a second step, the energy of the two electronic states is evaluated for each one of the structures determined in the first step using each of the exchange–correlation potential and the results for the triplet–singlet gap reported in Table 3 in a matrix form, where rows report  $\Delta_{\text{vert}}$  and  $\Delta_{\text{adia}}$  predicted by a given potential at geometries predicted by a given method and columns report the values predicted by different potentials at a given geometry. Results arising from the range separated LC- $\omega$ PBE functional are not included in Table 3 because the predictions, with values in the 6500–7500 cm<sup>−1</sup> range, are too far from available experimental data.

From Table 3 it is clear that all explored density functionals lead to optimized geometry structures for the triplet and singlet — as represented by a BS solution — which are relatively close. In fact, the vertical, approximate adiabatic (not shown in Table 3) from eq 4 and adiabatic from eq 3 calculated triplet–singlet gap obtained by using the different optimized structures exhibit a quite small variation of at most 3%. This is an important result because it clearly indicates that the variation with the functional, evident in Tables 1 and 3, does not arise from a difference in the predicted optimized geometry of the triplet and BS states but has its origin in the functional itself. Another important consequence is that choosing a density functional optimized geometry to evaluate the energy by a more sophisticated method such as CASSCF, CASPT2, MRCI, or DDCI can, in principle, be a well justified strategy.

Regarding the point above, it is important to advert that the inherent spin contamination of BS solution may also introduce artifacts in the corresponding optimized geometry. This has

been recently discussed by Malrieu and Trinquier<sup>86</sup> and by Saito and Thiel<sup>87</sup> proposing also different procedures to overcome this problem. The approach of Malrieu and Trinquier<sup>86</sup> consists on an extrapolation of the geometry to obtain a better estimate of the minimum energy of the spin decontaminated singlet, whereas Saito and Thiel<sup>87</sup> develop analytical gradients for the solution from spin projection of the BS solution and found that the structure of the approximate singlet thus obtained has some differences with that of the BS solution. The present B3LYP/6-311G\*\* geometry for the BS solution matches the one of Saito and Thiel<sup>87</sup> up to 0.01 Å, as expected. Interestingly, the CASSCF(8,8)/6-31G\* and CASSCF(8,8)/aug-cc-pVTZ optimized geometries for the singlet state are almost identical and also match the one predicted by Saito and Thiel<sup>87</sup> using the AGAP correction on top of the B3LYP/6-311G\*\* geometry for the BS solution. Therefore, one can suggest using the CASSCF(8,8) geometry to obtain an estimate of the effect of spin contamination in the geometry of the BS solution. The results in Table 4 clearly

**Table 4. Adiabatic Triplet–Singlet ( $\Delta_{\text{adia}}$ ) Gap of *m*-Xylylene As Predicted from Different DFT-Based Methods<sup>a</sup>**

	$\Delta_{\text{adia}}$	
	geom CASSCF	geom B3LYP
B3LYP	4118	4133
M06	4559	4585
M06-2X	3531	3726
HSE	4530	4633

<sup>a</sup>The values have been obtained from calculations using the 6-311++G\*\* basis set and using either the optimized structures obtained at the CASSCF(8,8)/6-31G\* (column geom CASSCF) or B3LYP/6-311G\*\* (column geom B3LYP) levels.

indicate that the changes due to the incorrect geometry of the BS solution are quite small for B3LYP, and M06 indicating that with these functionals, the BS approach predicts structures for the open-shell singlet comparable to those predicted by explicitly correlated wave function methods. Interestingly, significant differences are found for M06-2X and HSE. Therefore, this is an effect to be considered in this type of studies. The  $\Delta_{\text{adia}}$  values calculated by the B3LYP and M06-2X functionals using the CASSCF(8,8) geometry for the open-shell singlet get closer to the experimental value. The variation is, however, small meaning that the use of DFT methods to predict the geometry for subsequent post-Hartree–Fock calculations in this type of systems represents a rather reliable

strategy. In the general case, however, one needs to be aware of possible inaccuracies caused by the artifact in the geometry predicted by the BS approach.

**3.3. Influence of Active Space in CASCI, CASSCF, DDCI, and MRSDCI Calculations.** From results in previous subsections it is clear that it is desirable to validate the functional chosen which can be done either by comparison to experiment or by accurate ab initio wave function-based calculations. In the present subsection we explore the performance of some of the well-known wave function methods such as CASSCF, DDCI, and MR(SD)CI calculations. In particular, we explore the effect of the active space dimension in the CASSCF calculations and the influence of the orbitals chosen to carry out DDCI and MRSDCI calculations.

Table 5 summarizes results for  $\Delta_{\text{vert}}$  obtained with the several wave function-based methods using different sets of optimized orbitals obtained by means of CASSCF(*n,n*)/6-31G\*\* (*n* = 2, 4, 6, 8) where *n* = 2 corresponds to the minimal active space and *n* = 8 to the full  $\pi$  valence. These calculations are carried out at the geometry obtained at the CASSCF(8,8)/6-31G\* level. Similar results are obtained when using the geometry predicted by CASSCF(8,8)/6-311++G\*\* indicating that the problems described below cannot be attributed to structural effects. In the light of the work by Suaud et al.<sup>28</sup> on the effect of the orbitals we have computed  $\Delta_{\text{vert}}$  with the DDCI2, a variant of DDCI including all single excitation but only double excitations out of the CAS with two degrees of freedom (1h–1p, 2h, or 2p), the full DDCI, and MRSDCI with different sets of orbitals. Thus, the DDCI2, DDCI, and MRSDCI calculations use a complete active space configuration interaction (CASCI) with two electrons in two orbitals—hereafter referred to as CASCI(2,2)—as reference space for the subsequent CI-type calculations but with the natural orbitals obtained from CASSCF calculations using active spaces of increasing size. Moreover, the DDCI2, DDCI, and MRSDCI calculations are repeated using the orbitals corresponding to CASSCF calculations for the triplet, the singlet, or of state-specific type. Here, a caveat is necessary: strictly speaking, the DDCI calculations are fully justified when the same set of orbitals is used for the two states of interest, even though computational experience shows that the effect of the orbitals is most often not so crucial. In the forthcoming discussion we will show that this is not the case for MBDQM.

The first row of Table 5 reports the results of CASCI(*n,n*) calculations and different sets of orbitals. Note that, except in the case of state-specific results in the rightmost column, this is different from CASSCF since the orbitals of the triplet or of the

**Table 5. Vertical Triplet–Singlet ( $\Delta_{\text{vert}}$ ) Gap of *m*-Xylylene As Predicted from Different Wave Function-Based Methods Using Orbitals Obtained From CASSCF/6-31G\*\* Calculations<sup>a</sup>**

$\Delta_{\text{vert}}$	orbital set used											
	CASSCF for $^3B_2$				CASSCF for $^1A_1$				state-specific CASSCF			
	(2,2)	(4,4)	(6,6)	(8,8)	(2,2)	(4,4)	(6,6)	(8,8)	(2,2)	(4,4)	(6,6)	(8,8)
CASCI( <i>n,n</i> )	2643	5363	5061	5885	1119	2012	4441	5266	1632	3291	4757	5576
CASCI(2,2)+S	5823	6214	6283	6288	5122	5276	5530	5617	5903	6598	6824	6918
DDCI2	5364	5612	5620	5582	4835	4957	5150	5582	5612	6288	6480	6567
DDCI	3780	4629	5207	5714	3294	3366	3481	3543	5639	7589	8099	8342
MRSDCI	2511	5012	6825	8541	1299	1452	1764	1942	2300	2775	2218	1916

<sup>a</sup>Except for the CASCI(*n,n*) values, the orbitals correspond to CASSCF calculations of increasing size but taking the CASCI(2,2) as reference for subsequent calculations. The CASCI results of the first row, however, are consistent with the active space used in the CASSCF calculations. All calculations have been carried out using the CASSCF(8,8)/6-31G\*\* geometry of the triplet state. All values are in  $\text{cm}^{-1}$ .

**Table 6. Vertical and Adiabatic Triplet–Singlet ( $\Delta_{\text{vert}}$  and  $\Delta_{\text{adia}}$ ) Gap of *m*-Xylylene As Predicted from Different CASSCF and MRMP Methods with the CAS(8,8)<sup>a</sup>**

cm <sup>-1</sup>	B3LYP		HSE		M06		CASSCF		$\mu \pm \sigma$	
	$\Delta_{\text{vert}}$	$\Delta_{\text{adia}}$	$\Delta_{\text{vert}}$	$\Delta_{\text{adia}}$	$\Delta_{\text{vert}}$	$\Delta_{\text{adia}}$	$\Delta_{\text{vert}}$	$\Delta_{\text{adia}}$	$\Delta_{\text{vert}}$	$\Delta_{\text{adia}}$
CASSCF	5649	4892	5576	4817	5743	4915	5576	4482	5636 $\pm$ 69	4776 $\pm$ 174
MRMP	4622	4216	4576	4198	4678	4240	4577	4254	4613 $\pm$ 42	4227 $\pm$ 22

<sup>a</sup>The values have been obtained from calculations using the 6-31G\*\* basis set and the optimized structure either for triplet or singlet, obtained with the 6-311G\*\* basis set for the DFT-based methods and 6-31G\* for CASSCF. The different columns indicate the origin of the geometry and the rows report calculated values at the different structures. Mean values ( $\mu$ ) and standard deviation ( $\sigma$ ) are provided in the rightmost columns.

singlet are used to carry out the CASCI for the two states. The CASCI(*n,n*) results show that the effect of orbitals is dramatic. The triplet–singlet gap obtained from the orbitals of the triplet is very different from the value obtained from the orbitals of the singlet, and both are different from the result predicted from state-specific orbitals. Moreover, for a given choice of orbitals, the CASCI(*n,n*) results show a tremendous dependence on the choice of the active space, and only the CASCI(8,8) results arising from the orbitals obtained with CASSCF(8,8) show an onset of minimum stability, although the result still exhibits a large (66%) error with respect to experiment. This implies that dynamical electron correlation plays an essential role and also explains the difficulty to reduce the physics to the CAS(2,2) space evidenced in the recent work of Suaud et al.<sup>28</sup>

Electron correlation effects out of the CAS(2,2) reference space can be accounted for by including the single or single and double excitations out of the Slater determinants defining the CAS. This leads to the CASCI(2,2)+S and MR(SD)CI methods, respectively, whereas DDCI2 and DDCI represent suitable approximations to the MR(SD)CI with a smaller CI expansion. The CASCI(2,2)+S and DDCI2 methods (second and third row of Table 5) exhibit some stability with respect to the electronic state chosen to obtain the orbital set and with respect the dimension of the CAS. However, the results thus obtained do not represent any improvement with respect to the CASCI(8,8) results. Clearly, these two methods are not able to include the differential correlation effects.

Results from DDCI are also dependent on whether the orbitals are obtained from the triplet or singlet state. The DDCI calculations from state-specific orbitals lead to the worse results, which is not surprising since, rigorously, the DDCI conditions are only fulfilled when the CI expansions are built from the same orbital set. Interestingly, the DDCI calculations corresponding to the orbitals obtained from the singlet state are stable and do not depend on the size of the CAS used to obtain the orbitals and are very close to experiment. However, the agreement is purely fortuitous since DDCI should be a good approximation to MR(SD)CI which includes all single and double excitations in a variational way and, hence, the 2h–2p missing in the DDCI expansion. However, results in the bottommost row of Table 5 clearly show that the CAS(2,2) description does not provide a good zero-order reference irrespective of whether the orbitals are obtained from CASSCF calculations using a large set or not. One can claim that the failure of MRSDCI calculations is the lack of size consistency which is inherent to any truncated configuration interaction method. Note, however, that while size consistent effects clearly show up when dealing with bond breaking, its effect is almost negligible when dealing with electronic excitations. Therefore, one comes to the conclusion that the minimal CAS reference space is inadequate. This is in agreement with the findings of Suaud et al.<sup>28</sup> showing that the CAS(2,2) description is

only partly recovered upon use of natural orbitals iteratively obtained from DDCI calculations using the CAS(2,2) as reference space. This procedure is, however, not straightforward, and alternative approaches are desirable. This will be discussed in the next subsection.

**3.4. Influence of Geometry in the CASSCF and MRMP Calculations.** The discussion above and the results of Suaud et al.<sup>28</sup> about the inadequacy of a CAS(2,2) as reference, unless using iterative natural orbitals, imply that one should rely on a larger active space. The logical choice is the full  $\pi$  valence CAS(8,8) which is too large to be employed as reference in MR(SD)CI and even in DDCI calculations. This leaves one with two choices to include dynamical correlation effects: take into account the effect of single and double excitations out of the CAS by second-order perturbation theory or rely on some selection criterion to build the reference space. Here, we will analyze in detail the first option by using the MRMP method of Hirao<sup>67,67</sup> as implemented in GAMESS<sup>76,77</sup> which is similar to the CASPT2 method employed by Hrovat et al.<sup>23</sup> The last authors reported a quite accurate value, although the limited basis set (6-31G\*) and the CASSCF(8,8) were used which seem to leave room for improvement.

The results in subsection 3.2 suggest that using a geometry obtained from a DFT-based method in the MRMP calculations may be a good choice. Table 6 reports the  $\Delta_{\text{vert}}$  and  $\Delta_{\text{adia}}$  values calculated with CASSCF and MRMP using the 6-31G\*\* basis set at the B3LYP, M06, and HSE geometries obtained with the 6-311++G\*\* basis set and also with the CASSCF geometry obtained with the smaller 6-31G\*. Except for the case of  $\Delta_{\text{adia}}$  using the CASSCF geometry which can be easily understood from the inability of the CASSCF to describe the geometry of the singlet excited state, the CASSCF and MRMP values appear to be very stable and almost unaffected by the choice of the geometry. This confirms the prediction in subsection 3.2 that the use of the geometry predicted by a reliable DFT-based method is a good alternative. We close this subsection by noting that the MRMP value of roughly 4200 cm<sup>-1</sup> is in good agreement with the CASPT2 calculations of Hrovat et al.<sup>23</sup> but is still 25% in error with respect to experiment.

**3.5. Influence of Basis Set in the CASSCF and MRMP Calculations.** It is well recognized that basis set quality is crucial when the property of interest strongly depends on electron correlation effects. To clarify the effect of the basis set in the MRMP calculations two different additional sets of calculations have been carried out. In the first one, the geometry is obtained at the CASSCF/6-31G\* and the basis set is increased up to 6-311++G\*\* (Table 7), whereas in the second one the geometry is obtained at the CASSCF level, but at each of the basis sets, explored and correlation consistent basis sets are also included (Table 7).

Analysis of the results in Tables 7 and 8 shows that while the effect of enlarging the basis set is not large, there is a systematic



**Table 7. Vertical and Adiabatic Triplet–Singlet ( $\Delta_{\text{vert}}$  and  $\Delta_{\text{adia}}$ ) Gap of *m*-Xylylene As Predicted From CASSCF and MRMP with the CAS(8,8) Using Basis Sets of Increasing Size<sup>a</sup>**

cm <sup>-1</sup>	6-31g*		6-31g**		6-311++g**	
	$\Delta_{\text{vert}}$	$\Delta_{\text{adia}}$	$\Delta_{\text{vert}}$	$\Delta_{\text{adia}}$	$\Delta_{\text{vert}}$	$\Delta_{\text{adia}}$
CASSCF	5593	4501	5576	4482	5533	4432
MRMP	4600	4261	4577	4254	4349	4097

<sup>a</sup>In order to separate geometric effects, all values have been computed using the optimized structure as obtained with the CASSCF/6-31G\* approach.

improvement of the calculated result. However, even for the largest basis set, the final MRMP value for the adiabatic transition still exhibits a difference of 780 cm<sup>-1</sup> with respect to experiment with a residual error of 23%, which is not so different from the CASPT2/6-31G\* result of Hrovat et al.<sup>23</sup> Thus, the present results seem to indicate that further improvement requires either enlarging the dimension of the CAS or going to higher orders of perturbation theory. Increasing the dimension of the CAS becomes difficult both computationally and conceptually since once all  $\pi$  orbitals have been considered as active, one is left with the full valence CAS which will imply 40 active orbitals and 40 electrons. Going to higher orders of perturbation theory can in principle be achieved by DDCI, but the dimension of the resulting matrix makes this almost impossible. A last possibility consists of selecting some determinants in the CAS as references and carrying out MRSDCI calculations. A series of selected CI calculations have been carried out with the reference determinants chosen on the basis of the extent of their contributions to the CASSCF wave function. This set of calculations employs the 6-31G\*\* basis set and the geometry obtained at the CASSCF/6-311++G\*\* level and includes as reference the determinants in the CAS(8,8)+S wave function with contributions up to 0.03 or 0.09%. The largest reference space thus constructed contains 18 determinants. Unfortunately, the results for the vertical and adiabatic transitions are not stable with respect to the selection threshold which closes this way.

#### 4. GENERAL DISCUSSION

The systematic study presented in the previous sections illustrates how difficult it is to obtain an accurate result for the triplet–singlet gap of MBDQM and also offers some interesting conclusions and computational strategies for similar systems. For instance, the results of DFT-based calculations appear to be quite robust, and the dependence with respect to the basis set quality and to the molecular geometry is quite small. The main problem here is the dependence with respect to the choice of the exchange–correlation functional. In absence of experimental results it is difficult to assess the

accuracy of the different functionals. However, the fact that experimental results are available for MBDQM facilitates this issue. Clearly, the calculated value of 3607 cm<sup>-1</sup> in Table 2 for the adiabatic transitions predicted by the M06-2X functional within the extended 6-311++G(3df,3pd) basis set are those closest to experiment with an absolute error of 249 cm<sup>-1</sup>, or 7% error, only. The agreement becomes even more satisfactory if one considers the value obtained using the CASSCF(8,8)/aug-cc-pVTZ geometry for the triplet and singlet state. These calculations can be regarded as a way to estimate the spin contamination in the geometry on the BS solution,<sup>86,87</sup> as indicated above. The M06-2X calculated value using these geometries is of 3531 cm<sup>-1</sup> (Table 4) which implies an absolute error of 173 cm<sup>-1</sup> or 5%. Let us now consider the B3LYP functional which most often represents the default choice. Interestingly, the absolute error of B3LYP for the  $\Delta_{\text{adia}}$  transition in Table 2 is of 769 cm<sup>-1</sup>, predicted from the corresponding optimized triplet and BS solutions, is only slightly smaller than the one predicted by MRMP out of a CASSCF(8,8) wave function and with a rather extended basis set. This is a clear indication that singlet–triplet gaps predicted by DFT-based calculations within the BS approach are reliable, although the choice of the exchange–correlation functional remains a big issue. Note, in passing by, the  $\Delta_{\text{apadia}}$  values always deviate more from experiment which is not surprising given the approximations involved.

One can claim that more advanced functionals of the Minnesota can provide values numerically closer to the experimental value. To explore this possibility, an additional set of calculations has been carried out with the recently proposed range-separated hybrid nonseparable meta-GGA MN12-SX functional of Peverati and Truhlar.<sup>88</sup> The vertical and adiabatic triplet–singlet gaps predicted with this functional using the 6-311++G\*\* basis set, and the corresponding optimized geometries are 3985 and 3620 cm<sup>-1</sup> which are close to the equivalently obtained M06-2X values (4142 and 3615 cm<sup>-1</sup>), indicating that M06-2X and MN12-SX provide a similar description.

In order to further analyze the predictions from M06-2X and B3LYP, we computed the electron affinity of MBDQM which is also available from the NIPES experiments of Wentholt et al.<sup>22</sup> Using the largest 6-311++G(3df,3pd) basis set, the M06-2X and B3LYP calculations have been carried out for the vertical and adiabatic electron affinity using the optimized geometries of the neutral diradical (triplet) and anion (doublet). In a subsequent step, thermal corrections to energy and enthalpy at the temperature at which experiments have been carried out have been accounted for using the thermochemistry features implemented in Gaussian09. The calculated results, summarized in Table 9, reveal that both B3LYP and M06-2X predict values which are in very good agreement with experiment. The adiabatic values with zero-point corrections being considerably accurate (0.922 and 0.927 for B3LYP and M06-2X,

**Table 8. Vertical and Adiabatic Triplet–Singlet ( $\Delta_{\text{vert}}$  and  $\Delta_{\text{adia}}$ ) Gap of *m*-Xylylene As Predicted From CASSCF and MRMP with the CAS(8,8) Using Basis Sets of Increasing Size and the Corresponding CASSCF Geometry Optimized with Each Basis Set**

cm <sup>-1</sup>	6-31g*		6-311++g**		aug-cc-pVDZ		aug-cc-pVTZ	
	$\Delta_{\text{vert}}$	$\Delta_{\text{adia}}$	$\Delta_{\text{vert}}$	$\Delta_{\text{adia}}$	$\Delta_{\text{vert}}$	$\Delta_{\text{adia}}$	$\Delta_{\text{vert}}$	$\Delta_{\text{adia}}$
CASSCF	5593	4501	5531	4433	5535	4455	5585	4473
MRMP	4600	4261	4349	4110	4283	4102	4279	4138



**Table 9.** Calculated Vertical ( $EA_{\text{ver}}$ ), Adiabatic ( $EA_{\text{adia}}$ ), and Adiabatic Plus Zero-Point Corrections ( $EA_{\text{adia+Z}}$ ) Electron Affinity of *m*-Xylylene As Predicted from B3LYP and M06-2X DFT-Based Methods Using the 6-311++G(3df,3pd) Basis Set

eV	$EA_{\text{ver}}$	$EA_{\text{adia}}$	$EA_{\text{adia+Z}}$
B3LYP	0.843	0.784	0.922
M06-2X	0.875	0.800	0.927
experiment <sup>22</sup>		0.919 ± 0.008	

respectively) with a <1% error with respect to the 0.919 ± 0.008 eV experimental value;<sup>22</sup> which is a remarkable achievement for the calculation of such an elusive property. Therefore, one could conclude that the prediction of triplet–singlet gaps in this type of systems is reasonably well described, at least from the numerical point of view, by hybrid functionals.

The results of the present systematic study concerning the use of explicitly correlated wave function methods are somewhat disappointing, evidencing the difficulty to obtain values which reduce the 22% error with respect to experiment corresponding to the CASPT2 published by Hrovat et al.<sup>23</sup> more than 15 years ago. Nevertheless, a number of important conclusions emerged. First, this is an example where the minimal CAS(2,2) description is hardly correct, needing to rely on iterative natural orbitals from a DDCI calculation out of the CASSCF(2,2) function as shown by Suaud et al.<sup>28</sup> In the present work we attempted to recover the minimal physically grounded CAS(2,2) by relying instead on the orbitals from larger active spaces. Unfortunately, the CASSCF(8,8) calculations lead to orbitals for the triplet and singlet which are very different. This has the consequence that DDCI calculations also fail and even MR(SD)CI out of a CAS(2,2) built from the orbitals of CASSCF(8,8) fail to produce reasonable results. Therefore, one has to rely either on costly and tedious iteratively obtained natural orbitals or on second-order perturbation theory with the CASSCF while using CAS(8,8) as reference. The two approaches lead to similar results, although present results hardly improve over the CASPT2 description of Hrovat et al.<sup>23</sup> though the MRMP scheme is perhaps more adequate and larger basis sets are used.

From the positive point of view, MRMP calculations carried out at different geometries, including those obtained with several density functionals, are quite stable indicating that this is indeed a good option. The effect of the basis set is not unexpectedly larger, but even with quite large basis sets including those of correlation consistent type, the calculated triplet–singlet gap of MBDQM is still large, at about 22% (4097 cm<sup>-1</sup> with 6-311++G\*\* basis set). The difficulty of the wave function-based methods in describing the triplet–singlet gap arises quite unequivocally from dynamical correlation effects which cannot be recovered unless an even larger CAS is used, but this becomes computationally prohibitive. This is confirmed by the results obtained for the electron affinity of MBDQM. The adiabatic value predicted by CASSCF calculations with CAS(8,8) and CAS(9,8) for the triplet state of the neutral molecule and doublet state of the anion at the corresponding CASSCF geometry optimized with the 6-311++G\*\* basis set is qualitatively incorrect. Including dynamical correlation through MRMP recovers the correct sign but the calculated value of 0.132 only represents a too poor approximation to the experimental value of 0.919 ± 0.008 eV<sup>22</sup> and also far from the B3LYP and M06-2X corresponding

values in Table 9. Clearly, the CAS(8,8)/CAS(9,8) description is insufficient, and the basis set is also too limited to account for the differential electronic dynamical correlation.

## 5. CONCLUSIONS

The triplet–singlet gap of MBDQM has been computed by a variety of density functional and wave function-based methods in an attempt to provide a guide in the study of similarly large systems for which the wave function methods become unmanageable. The effect of the basis set and geometry has been separately explored, and a number of conclusions have been reached. These are given below.

- (1) Beyond a certain reasonable quality, the triplet–singlet gap of MBDQM predicted by different density functionals does not depend too much on the basis set. Moreover, the geometries predicted by the different functionals are fairly consistent, which means that to investigate the effect of the functional one can use the geometry for the triplet and singlet predicted by any of these functionals.
- (2) The triplet–singlet energy gap of MBDQM predicted by different density functionals strongly depends on the choice of the functional to the point that results from the range-separated LC- $\omega$ PBE method become unacceptable, probably indicating that the standard parameters for range separation are not at all appropriate for this type of highly conjugated systems. The M06-2X meta-GGA functional provides the best comparison to experiment, and the performance of B3LYP is also good. This good numerical behavior is confirmed by the calculation of the electron affinity which, for both functionals, is in very good agreement with experiment. Nevertheless, the dependence on the functional cannot be ignored.
- (3) The use of the BS optimized geometry to compute the adiabatic singlet–triplet gap does not represent a serious problem, although improved agreement with experiment can be obtained by using a more accurate geometry.
- (4) The physically meaningful CAS(2,2) description of the triplet–singlet gap of MBDQM cannot be recovered by simply expanding the CAS to the full  $\pi$  valence. In addition, DDCI and MRSDCI values obtained using a CAS(2,2) as reference, but the orbitals from larger CASSCF up to CAS(8,8) are found to lie in a too broad range to validate this strategy.
- (5) MRPT calculations out of the CASSCF(8,8) provide a semiquantitative prediction of the triplet–singlet gap of MBDQM especially when using the larger basis sets but give only a modest improvement over the previous CASPT2 values. This happens in spite of the fact that the uncontracted nature of the MRMP scheme facilitates a rescaling of the contribution of CAS determinants in the first order perturbed wave function.
- (6) MRPT calculations using the geometry that has been optimized by a given hybrid or meta-GGA functional provide similar values of the triplet–singlet gap of MBDQM, thereby suggesting that this would be a considerably useful strategy.
- (7) Finally, the fact that MRCI and MRMP systematically overestimate the triplet–singlet gap may indicate that basis set and reference space requirements are not fulfilled or, alternatively, that the experimental value is slightly affected by the experimental conditions. Note

that the NIPES experiment is carried out in a helium environment at 175–185 K<sup>22</sup> and some energy-transfer mechanism is needed to explain the non-Franck–Condon character of the NIPES spectrum of MBDQM.

The problems encountered here for the wave function description of MBDQM are reminiscent of the previous work by Nachtigall and Jordan<sup>14–16</sup> as well as by Cramer and Smith<sup>17</sup> on tetramethyleneethane and trimethylenemethane, respectively, even if the former represents a different case since it involves a disjoint diradical where two allyl radical moieties are connected through their nodal atoms. These authors concluded that an accurate many-body treatment of a diradical becomes tricky, with somewhat erratic behavior noticed from one methodology to another and sometimes with basis size. The theoretical level of methodology can be raised but with a huge concomitant increase in computing efforts. The present work on a nontrivial diradical provides a convenient and useful guide for what is to be expected from a systematic many-body study of magnetic interactions in largely conjugated organic radicals that may have at least one aromatic ring. Finally, one must warn that previous results of Valero et al.<sup>89</sup> on  $\alpha$ -4-dehydrotoluene and biverdazyl radicals suggest that the performance of a given functional, hybrid, or meta GGA, with respect to the triplet–singlet gap is also system dependent and comparison to experiment or to similar systems becomes unavoidable before choosing a given method.

## ■ ASSOCIATED CONTENT

### ■ Supporting Information

Tables S1–S9 of optimized coordinates, energies, computed S2 expectation values, and calculated S–T energy gaps from both UDFT and WF-based methods. More on UDFT: Optimization – Log file 1–4; Single-point calculation – Log file 5–8; Optimization for doublet – Log file 9–12; Calculation of single point triplet and BS of diradical by taking optimized anion doublet – Log file 13–16; Frequency calculations diradical and electron affinity from Log file 17–20. This material is available free of charge via the Internet at <http://pubs.acs.org>.

## ■ AUTHOR INFORMATION

### Corresponding Author

\*E-mail: [francesc.illas@ub.edu](mailto:francesc.illas@ub.edu).

### Notes

The authors declare no competing financial interest.

## ■ ACKNOWLEDGMENTS

The authors are indebted to Prof. Jean Paul Malrieu and Dr. Nathalie Guihéry for interesting discussions regarding the electronic structure of *m*-xylylene. This work has been supported by Indo-Spain Collaborative Program in Science – Nanotechnology (DST Grant INT-Spain-P42-2012 and Spanish Grant PRI-PIBIN-2011-1028) and, in part, by Spanish MICINN through research grants FIS2008-02238 and CTQ2012-30751 and by Generalitat de Catalunya through grants 2009SGR1041, XRQTC. Furthermore, S.N.D. and A.K.P. are grateful to DST Grant SR-S1-PC-19-2010 for financial support of this work, and F.I. acknowledges additional financial support through the 2009 ICREA Academia Award for Excellence in University Research. Finally, we must acknowledge the contribution of two anonymous reviewers which has resulted in a much improved article.

## ■ REFERENCES

- (1) Platz, M. S.; *Diradicals*; Borden, W. T., Ed.; Wiley-Interscience: New York, 1982; pp 1–343.
- (2) Dougherty, D. A. *Kinetics and Spectroscopy of Carbenes and Biradicals*; Platz, M. S., Ed.; Plenum: New York, 1990; p 117.
- (3) Lewis, G. N.; Lipkin, D. *J. Am. Chem. Soc.* **1942**, *64*, 2801.
- (4) Porter, G. *Proc. R. Soc. London* **1950**, *A200*, 284.
- (5) Biewer, M. C.; Biehn, C. R.; Platz, M. S.; Despres, A.; Migirdicyan, E. *J. Am. Chem. Soc.* **1991**, *113*, 616.
- (6) Wenthold, P. C.; Lineberger, W. C. *Acc. Chem. Res.* **1999**, *32*, 597.
- (7) Rajca, A. *Chem. Rev.* **1994**, *94*, 871.
- (8) Iwamura, H.; Koga, N. *Acc. Chem. Res.* **1993**, *26*, 346.
- (9) Borden, W. T.; Davidson, E. R. *J. Am. Chem. Soc.* **1977**, *99*, 4587.
- (10) Ovchinnikov, A. A. *Theor. Chim. Acta* **1978**, *47*, 297.
- (11) Lieb, E. H. *Phys. Rev. Lett.* **1989**, *62*, 201.
- (12) Trindle, C.; Datta, S. N. *Int. J. Quantum Chem.* **1996**, *57*, 781.
- (13) Trindle, C.; Datta, S. N.; Mallik, B. J. *Am. Chem. Soc.* **1997**, *119*, 12947.
- (14) Nachtigall, P.; Jordan, K. D. *J. Am. Chem. Soc.* **1992**, *114*, 4143.
- (15) Nachtigall, P.; Dowd, P.; Jordan, K. D. *J. Am. Chem. Soc.* **1992**, *114*, 4741.
- (16) Nachtigall, P.; Jordan, K. D. *J. Am. Chem. Soc.* **1993**, *115*, 270.
- (17) Cramer, C. J.; Smith, B. A. *J. Phys. Chem.* **1996**, *100*, 9664.
- (18) Moreira, I.; de, P. R.; Illas, F. *Phys. Chem. Chem. Phys.* **2006**, *8*, 1645.
- (19) Neese, F. *Coord. Chem. Rev.* **2009**, *253*, 526.
- (20) Bencini, A.; Totti, F. *J. Chem. Theory Comput.* **2009**, *5*, 144.
- (21) Wright, B. B.; Platz, M. S. *J. Am. Chem. Soc.* **1983**, *105*, 628.
- (22) Wenthold, P. G.; Kim, J. B.; Lineberger, W. C. *J. Am. Chem. Soc.* **1997**, *119*, 1354.
- (23) Hrovat, D. A.; Murcko, M. A.; Lahti, P. M.; Borden, W. T. *J. Chem. Soc., Perkin Trans. 2* **1998**, *5*, 1037.
- (24) Lineberger, W. C.; Borden, W. T. *Phys. Chem. Chem. Phys.* **2011**, *13*, 11792.
- (25) Fort, R. C., Jr.; Getty, S. J.; Hrovat, D. A.; Lahti, P. M.; Borden, W. T. *J. Am. Chem. Soc.* **1992**, *114*, 7549.
- (26) Wang, T.; Krylov, A. I. *J. Chem. Phys.* **2005**, *123*, 104304.
- (27) de Graaf, C.; Sousa, C.; Moreira, I.; de, P. R.; Illas, F. *J. Phys. Chem. A* **2001**, *105*, 11371.
- (28) Suaud, N.; Ruamps, R.; Guihéry, N.; Malrieu, J. P. *J. Chem. Theory Comput.* **2012**, *8*, 4127.
- (29) Datta, S. N.; Jha, P. P.; Ali, E. M. *J. Phys. Chem. A* **2004**, *108*, 4087.
- (30) Ali, E. M.; Datta, S. N. *J. Phys. Chem. A* **2006**, *110*, 2776.
- (31) Ali, E. M.; Datta, S. N. *J. Phys. Chem. A* **2006**, *110*, 13232.
- (32) Latif, I. A.; Hansda, S.; Datta, S. N. *J. Phys. Chem. A* **2012**, *116*, 8599.
- (33) Pal, A. K.; Hansda, S.; Datta, S. N.; Illas, F. *J. Phys. Chem. A* **2013**, *117*, 1773.
- (34) Datta, S. N.; Pal, A. K.; Hansda, S.; Latif, I. A. *J. Phys. Chem. A* **2012**, *116*, 3304.
- (35) Mitani, M.; Mori, H.; Takano, Y.; Yamaki, D.; Yoshioka, Y.; Yamaguchi, K. *J. Chem. Phys.* **2000**, *113*, 4035.
- (36) Mitani, M.; Yamaki, D.; Takano, Y.; Kitagawa, Y.; Yoshioka, Y.; Yamaguchi, K. *J. Chem. Phys.* **2000**, *113*, 10486.
- (37) Mitani, M.; Takano, Y.; Yoshioka, Y.; Yamaguchi, K. *J. Chem. Phys.* **1999**, *111*, 1309.
- (38) Ditchfie, R.; Hehre, W. J.; Pople, J. A. *J. Chem. Phys.* **1971**, *54*, 724.
- (39) Hehre, W. J.; Ditchfie, R.; Pople, J. A. *J. Chem. Phys.* **1972**, *56*, 2257.
- (40) Dunning, T. H., Jr. *J. Chem. Phys.* **1989**, *90*, 1007.
- (41) Hariharan, P. C.; Pople, J. A. *Theor. Chim. Acta* **1973**, *28*, 213.
- (42) Clark, T.; Chandrasekhar, J.; Spitznagel, G. W.; Schleyer, P. V. R. *J. Comput. Chem.* **1983**, *4*, 294.
- (43) Frisch, M. J.; Pople, J. A.; Binkley, J. S. *J. Chem. Phys.* **1984**, *80*, 3265.
- (44) Kendall, R. A.; Dunning, T. H., Jr.; Harrison, R. J. *J. Chem. Phys.* **1992**, *96*, 6796.

- (45) Becke, A. D. *J. Chem. Phys.* **1993**, *98*, 5648.
- (46) Zhao, Y.; Truhlar, D. G. *J. Chem. Phys.* **2006**, *125*, 194101.
- (47) Zhao, Y.; Truhlar, D. G. *J. Phys. Chem. A* **2006**, *110*, 13126.
- (48) Zhao, Y.; Truhlar, D. G. *Theor. Chem. Acc.* **2008**, *120*, 215.
- (49) Heyd, J.; Scuseria, G. E.; Ernzerhof, M. *J. Chem. Phys.* **2003**, *518*, 8207; *ibid* **2006**, *124*, 219906(E).
- (50) Vydrov, O. A.; Scuseria, G. E. *J. Chem. Phys.* **2006**, *125*, 234109.
- (51) Illas, F.; Moreira, I.; de, P. R.; Bofill, J. M.; Filatov, M. *Phys. Rev. B* **2004**, *70*, 132414.
- (52) Illas, F.; Moreira, I.; de, P. R.; Bofill, J. M.; Filatov, M. *Theor. Chem. Acc.* **2006**, *115*, 587.
- (53) Filatov, M.; Shaik, S. *Chem. Phys. Lett.* **1998**, *288*, 689.
- (54) Filatov, M.; Shaik, S. *Chem. Phys. Lett.* **1999**, *304*, 429.
- (55) Slipchenko, L. V.; Krylov, A. I. *J. Chem. Phys.* **2002**, *117*, 4694.
- (56) Moreira, I.; de, P. R.; Costa, R.; Filatov, M.; Illas, F. *J. Chem. Theory Comput.* **2007**, *3*, 764.
- (57) Valero, R.; Illas, F.; Truhlar, D. G. *J. Chem. Theory Comput.* **2011**, *7*, 3523.
- (58) Noodleman, L. *J. Chem. Phys.* **1981**, *74*, 5737.
- (59) Noodleman, L.; Davidson, E. R. *J. Chem. Phys.* **1986**, *109*, 131.
- (60) Noodleman, L.; Peng, C. Y.; Case, D. A.; Mouesda, J. M. *Coord. Chem. Rev.* **1995**, *144*, 199.
- (61) Caballol, R.; Castell, O.; Illas, F.; Malrieu, J. P.; Moreira, I.; de, P. R. *J. Phys. Chem. A* **1997**, *101*, 7860.
- (62) Yamaguchi, K.; Takahara, Y.; Fueno, T.; Nasu, K. *Jpn. J. Appl. Phys.* **1987**, *26*, L1362.
- (63) Yamaguchi, K.; Jensen, F.; Dorigo, A.; Houk, K. N. *Chem. Phys. Lett.* **1988**, *149*, 537.
- (64) Yamaguchi, K.; Takahara, Y.; Fueno, T.; Houk, K. N. *Theor. Chim. Acta* **1988**, *73*, 337.
- (65) Hirao, K. *Int. J. Quantum Chem.* **1992**, *S26*, 517.
- (66) Hirao, K. *Chem. Phys. Lett.* **1992**, *190*, 374.
- (67) Hirao, K. *Chem. Phys. Lett.* **1992**, *196*, 397.
- (68) Hirao, K. *Chem. Phys. Lett.* **1993**, *201*, 59.
- (69) Miralles, J.; Castell, O.; Caballol, R.; Malrieu, J. P. *Chem. Phys.* **1993**, *172*, 33.
- (70) Malrieu, J. P. *J. Chem. Phys.* **1967**, *47* (11), 4555.
- (71) Foresman, J. B.; Head-Gordon, M.; Pople, J. A.; Frisch, M. J. *J. Phys. Chem.* **1992**, *96*, 135.
- (72) Harrison, J. F. *Chem. Rev.* **2000**, *100*, 679.
- (73) Helgaker, T.; Coriani, S.; Jorgensen, P.; Kristensen, K.; Olsen, J.; Ruud, K. *Chem. Rev.* **2012**, *112*, 543.
- (74) Malrieu, J. P.; Caballol, R.; Calzado, C. J.; de Graaf, C.; Guihéry, N. *Chem. Rev.* in press, DOI: 10.1021/cr300500z.
- (75) Frisch, M. J.; Trucks, G. W.; Schlegel, H. B.; Scuseria, G. E.; Robb, M. A.; Cheeseman, J. R.; Scalmani, G.; Barone, V.; Mennucci, B.; Petersson, G. A.; Nakatsuji, H.; Caricato, M.; Li, X.; Hratchian, H. P.; Izmaylov, A. F.; Bloino, J.; Zheng, G.; Sonnenberg, J. L.; Hada, M.; Ehara, M.; Toyota, K.; Fukuda, R.; Hasegawa, J.; Ishida, M.; Nakajima, T.; Honda, Y.; Kitao, O.; Nakai, H.; Vreven, T.; Montgomery, J. A., Jr.; Peralta, J. E.; Ogliaro, F.; Bearpark, M.; Heyd, J. J.; Brothers, E.; Kudin, K. N.; Staroverov, V. N.; Kobayashi, R.; Normand, J.; Raghavachari, K.; Rendell, A.; Burant, J. C.; Iyengar, S. S.; Tomasi, J.; Cossi, M.; Rega, N.; Millam, N. J.; Klene, M.; Knox, J. E.; Cross, J. B.; Bakken, V.; Adamo, C.; Jaramillo, J.; Gomperts, R.; Stratmann, R. E.; Yazyev, O.; Austin, A. J.; Cammi, R.; Pomelli, C.; Ochterski, J. W.; Martin, R. L.; Morokuma, K.; Zakrzewski, V. G.; Voth, G. A.; Salvador, P.; Dannenberg, J. J.; Dapprich, S.; Daniels, A. D.; Farkas, Ö.; Foresman, J. B.; Ortiz, J. V.; Cioslowski, J.; Fox, D. J. *Gaussian 09*, revision A.1; Gaussian, Inc.: Wallingford, CT, 2009.
- (76) Schmidt, M. W.; Baldridge, K. K.; Boatz, J. A.; Elbert, S. T.; Gordon, M. S.; J. Jensen, H. S.; Koseki, N.; Matsunaga, K.; Nguyen, A.; Su, S.; Windus, T. L.; Dupuis, M. J.; Montgomery, A. J. *Comput. Chem.* **1993**, *14*, 1347.
- (77) Gordon, M. S.; Schmidt, M. W. 1167–1189, In *Theory and Applications of Computational Chemistry: the first forty years*; Dykstra, C. E., Frenking, G., Kim, K. S., Scuseria, G. E., Eds.; Elsevier: Amsterdam, 2005.
- (78) Ben Amor, N.; Maynau, D. *Chem. Phys. Lett.* **1998**, *286*, 211; CASDI program: Package developed at the Laboratoire de Chimie et Physique Quantiques, Université Paul Sabatier, Toulouse (France).
- (79) Aquilante, F.; de Vico, L.; Ferré, N.; Ghigo, G.; Malmqvist, P.-A.; Pedersen, T.; Pitonak, M.; Reiher, M.; Roos, B. O.; Serrano-Andrés, L.; Urban, M.; Varyazov, V.; Lindh, R. *J. Comput. Chem.* **2010**, *31*, 2240.
- (80) Andersson, K.; Malmqvist, P.-Å.; Roos, B. O.; Sadlej, A. J.; Wolinski, K. *J. Phys. Chem.* **1990**, *94*, 5483.
- (81) Andersson, K.; Malmqvist, P.-Å.; Roos, B. O. *J. Chem. Phys.* **1992**, *96*, 1218.
- (82) Angeli, C.; Cimiraglia, R.; Evangelisti, S.; Leininger, T.; Malrieu, J. P. *J. Chem. Phys.* **2001**, *114*, 10252.
- (83) Rivero, P.; Moreira, I.; de, P. R.; Illas, F.; Scuseria, G. E. *J. Chem. Phys.* **2008**, *129*, 184110.
- (84) Rivero, P.; Moreira, I.; de, P. R.; Scuseria, G. E.; Illas, F. *Phys. Rev. B* **2009**, *79*, 245129.
- (85) Johnson, B. G.; Gill, P. M. W.; Pople, J. A. *J. Chem. Phys.* **1993**, *98*, 5612.
- (86) Malrieu, J. P.; Trinquier, G. *J. Phys. Chem. A* **2012**, *116*, 8226.
- (87) Saito, T.; Thiel, W. *J. Phys. Chem. A* **2012**, *116*, 10824.
- (88) Peverati, R.; Truhlar, D. G. *Phys. Chem. Chem. Phys.* **2012**, *14*, 16187.
- (89) Valero, R.; Costa, R.; Moreira, I.; de, P. R.; Truhlar, D. G.; Illas, F. *J. Chem. Phys.* **2008**, *128*, 114103.